On properly integrating the electronic Raman and optical infra-red spectra of high temperature superconducting cuprate materials

2009 J. Phys.: Condens. Matter 21 495703

(http://iopscience.iop.org/0953-8984/21/49/495703)

J. Phys.: Condens. Matter **21** (2009) 495703 (10pp) doi:10.1088/0953-8984/21/49/495703

On properly integrating the electronic Raman and optical infra-red spectra of high temperature superconducting cuprate materials

John A Wilson

H H Wills Physics Laboratory, University of Bristol, Bristol BS8 1TL, UK

E-mail: john.a.wilson@bris.ac.uk

Received 29 May 2009, in final form 22 October 2009
Published 19 November 2009
Online at stacks.iop.org/JPhysCM/21/495703

Abstract

New electronic Raman and infra-red spectroscopy results from optimally and overdoped high temperature superconducting cuprate systems are interpreted in terms of the negative-U, boson–fermion crossover model. A distinction is made between those features which follow the condensate gap, $2\Delta(p)$, and those that are set by the local pair binding energy, $\mathcal{U}(p)$. The critical role of the doping level $p_c = 0.185$ is highlighted in conjunction with the question of developing quasiparticle incoherence, making connection here with recent transport and related results. $E \parallel c$ IR results for magnetic fields parallel and perpendicular to c prove particularly illuminating. The general scheme developed continues to embrace all experimental data very satisfactorily.

1. Introduction to boson–fermion negative-U crossover modelling of high temperature superconducting (HTSC) cuprates

It has been notoriously difficult to come to any consensus on the interpretation of the highly characteristic, low energy optical behaviour of the high temperature superconducting cuprates. It has long been evident here, as with all other of their properties, that in neither superconducting nor normal state do these materials behave as simple classical systems [1, 2]. There is self-evidently far too much abnormality for any conventionally based explanation to succeed in embracing all the observations. Not only is it necessary to fold suitably into the analysis now fairly routine matters like their proximity to the Mott transition and to a band structural saddle-point crossover, to their structural instability and charge striping, to their spin and charge density wave tendencies, but above all it is necessary to recognize the unusual strong scattering characterizing both normal and superconducting state alike. What is source to the displayed Marginal Fermi Liquid behaviour? It is very clear that properly tracking and understanding the course and causes of this novel scattering will carry one to the heart of the HTSC phenomenon [3]. Some have turned to phonon soft modes and others to spin fluctuations, each to considerable acclaim, but to the author it never has seemed that these phenomena are sufficiently unusual or extreme to bestow upon the cuprates their manifest uniqueness.

Now charge fluctuations in an inhomogeneous setting, such as is afforded by the present mixed-valent HTSC materials, in particular in view of their proximity to the Mott–Anderson transition, are a different matter. Coulomb interactions cover an altogether different energy scale. Of course this of itself is a problem, potentially negating their relevance. How can charge fluctuations be entertained in a near-Mott insulator? Surely, if given positive-U Hubbard energies ∼4 eV, one is obliged to project them out of the problem. Now this would indeed be the case were the HTSC systems homogeneous, but they are not, and furthermore it may well be true were the charge not directly engaged in chemical bonding, but it is. Not only are the electronic system and the lattice irrevocably one, interdependent, but within that whole all the various band and bond energies are able to respond individually and simultaneously, both up and down. Charge fluctuations have complex courses and often striking outcomes [4] and none more so than when quantum shell closure is involved.

In the present case of the mixed-valent cuprates [5], the double-loading charge fluctuations in question are adequately represented by the intervalence, three-unit process

$$^{9}\mathrm{Cu}_{\mathrm{II}}^{0} + {}^{9}\mathrm{Cu}_{\mathrm{II}}^{0} + {}^{8}\mathrm{Cu}_{\mathrm{III}}^{0} \longrightarrow {}^{8}\mathrm{Cu}_{\mathrm{II}}^{1+} + {}^{8}\mathrm{Cu}_{\mathrm{II}}^{1+} + {}^{10}\mathrm{Cu}_{\mathrm{III}}^{2-}.$$

Note the double loading occurs here into coordination units that nominally carry trivalent Madelung charging by virtue of local counter-cation substitution and/or excess interstitial oxygen content. Moreover the double loading brings the local, shell-filling, configuration $\mathrm{p}^6\mathrm{d}^{10}$, and in its trivalent setting the d^{10} shell then becomes greatly stabilized. The latter effect is not just atomic physics but the effect of the above new electron count upon the local cation/anion bonding interaction. The antibonding p/d hybridization that hitherto had held the chemical potential high at d^8, and even at d^9, now with d^{10} becomes terminated. The d^{10} closed shell is thereby freed to relax rapidly in energy to its new status, semi-core-like when uncharged, though here much distended, whilst the oxygen p states, no longer constituting stabilized partner within the dpσ bonding interaction, are freed to rise in energy up through the descending copper d-state set. The end product is that the local chemical potential at the doubly-loaded $\mathrm{Cu}_{\mathrm{III}}$ coordination unit, instead of being driven strongly upwards, actually finds itself back in close resonance with E_{F} as this runs across the surrounding delocalized, mixed-valent, Fermi sea. The local pair $\mathrm{e} + \mathrm{e} \rightarrow \mathrm{b}$ fluctuational creation stands in this way in near-resonance with E_{F} in the HTSC materials. The strong characteristic anisotropic scattering engendering Marginal Fermi Liquid behaviour is perceived by the author as being of the above origin in conjunction with the ensuing partner process of e-on-b scattering, i.e. of near-degenerate quasiparticles on local pairs [5]. The latter scattering is small-angle in form and it becomes dominant partner around $p(T_{\mathrm{c}}^{\mathrm{opt}})$, at the stage where local pair definition and lifetime are most advanced.

To arrive at this picture calls for a Hubbard negative-U value local to trivalent sites of -1.5 eV per electron [6], roughly the size of the d_{x2-y2} bandwidth. U takes its standard definition by reference to single loading—here the local trivalent condition $^{9}\mathrm{Cu}_{\mathrm{III}}^{1-}$—of

$$U = (E_{n+2} - E_{n+1}) - (E_{n+1} - E_n) = (E_{n+2} + E_n) - 2E_{n+1} \qquad \text{per pair.}$$

Within the mixed-valent environment of the HTSC cuprates the global level of E_{F} is largely dictated not by $^{9}\mathrm{Cu}_{\mathrm{III}}^{1-}$ but by the majority species $^{9}\mathrm{Cu}_{\mathrm{II}}^{0}$. This means that the negative-U state $^{10}\mathrm{Cu}_{\mathrm{III}}^{2-}$ will not find degeneracy with E_{F} unless and until $|U|$ per electron comes to possess roughly the bandwidth energy $\sim$ 1.5 eV (see figure 3 in [11]). Accordingly actual *binding* energies, cursive $\mathcal{U}$, for a local pair (per electron) are thus reached only as and when $|U|$ exceeds such a value.

The above value of Hubbard U of -1.5 eV per electron for trivalent sites in the HTSC materials is supported experimentally from a wide variety of laser pump–probe experimental results [7–10], discussed in [6, 10–12] by the current author, and from Little and co-worker's near-infra thermomodulation spectroscopy [13], discussed at length in [14]. As indicated above this value of $U \approx -1.5$ eV per electron is able to position the crucial state ($^{10}\mathrm{Cu}_{\mathrm{III}}^{2-}$) relating to resonance and successful boson–fermion crossover modelling at a small binding energy, cursive $\mathcal{U}$, amounting to ~ -50 meV ($\approx 2\Delta(0)$). The precise value of this small binding energy as a function both of p and of overall system covalency is on display, it is claimed by the present author in [15–17], in the scanning tunnelling spectroscopy experiments of Davis, Hanaguri and co-workers [18–20]. The detailed situation as a function of p I set out originally, when working from the Seebeck results, in figure 1 of [21]. The latter figure, now reproduced slightly modified as figure 1, indicates how the local pair level stands relative to the *absolute* binding level of $E_{\mathrm{F}}(p)$. The energies specified are extracted from figure 3 of [5a], itself deriving from the author's spectroscopic studies on transition metal compounds summarized in figure 7 of [22].

Careful distinction needs to be made in all this work between the evolution of $\mathcal{U}(p)$ and of $\Delta(p)$, the latter being the system-wide superconductive gap established over the entire system under the stimulus of the resonant pairs. ARPES, as with all other optical probes, records the convolution of the two features. In these HTSC cuprates local pair generation under e–e scattering arises most effectively from the saddle 'hot spots' to the zone corner (see figure 3 in [6]), whilst the bosons themselves, once created, likewise scatter most strongly from the heavy quasiparticles of the saddle regions. The anisotropy and form of these twin components to the resistive scattering as functions of T and p have recently been addressed again in [23] following Hussey *et al*'s detailed transport, angular magneto-resistance and de Haas–Shubnikov studies of HTSC systems [24–26]. While the negative-U state first drops below $E_{\mathrm{F}}(p)$ in the vicinity of $p = 0.27$, the optimal interaction between bosonic and fermionic subsystems does not arise until $p \approx 0.18$. This concentration of holes is optimal in the sense of providing a suitably localized milieu for the sustained number of superconducting pairs, n_{s}, to come to its highest value, as is made evident in muon spin resonance/penetration depth studies [27]. At this stage the condensation energy per carrier, as disclosed from electronic specific heat studies [28], arrives at its maximum value. Optimization of T_{c} is, on the other hand, not gained until the slightly smaller p value of 0.16. As a result of rapidly growing quasiparticle incoherence below $p = 0.18$, the greater locality and definition accruing to the local pair Madelung potential quickly become out-weighed by the falling coherent quasiparticle count. Because the binding energy $\mathcal{U}(p)$ goes on increasing into the underdoped 'pseudogap' regime it rapidly becomes decoupled from the fermionic subsystem, and from the size of $\Delta(p)$ secured for the overall superconducting state. This is the so-called gapping dichotomy [29], in which $\Delta(p)$ tracks $T_{\mathrm{c}}(p)$ and $n_{\mathrm{s}}(p)$, receding with the reduction in p count, whilst $|\mathcal{U}(p)|$ continues steadily to increase as p drops towards the Mott limit and the onset of antiferromagnetism. $\Delta_{\mathrm{o}}(p)$ is, note, ultimately prescribed through action in the nodal, 45° directions, whilst $\mathcal{U}(p)$, by contrast, being bound only towards the outer parts of the Brillouin zone, stands as an axial, saddle, or antinodal entity.

From this standpoint of what is underway in the HTSC cuprates, we may set about clarifying those hitherto perplexing details of the electronic Raman and IR optical spectra.

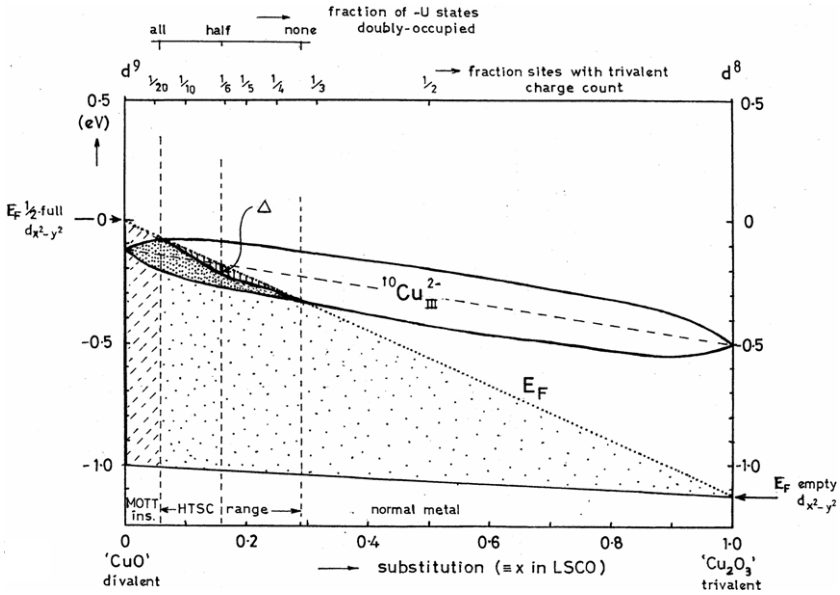

Figure 1. Slightly modified scale diagram taken from [21], indicating relative and absolute energies across the mixed-valent range from Cu_{II} to Cu_{III} of (i) the bottom of the σ^*pd_{x2-y2} band, (ii) the Fermi level, and (iii) the local pair fluctuational state $^{10}Cu_{III}^{2-}$. This state is shown (i) optimally resonant with E_F at $p = 0.16$, (ii) bound relative to $E_F(p)$ at $p = 0$ with antinodal binding energy $\mathcal{U} = 75$ meV, and (iii) fully unbound by $p = 0.28$ relative to E_F at that point. The width assigned to the local pair state derives from the intrinsic substitutional/interstitial disorder. For both limiting concentrations of $p = 0$ and 1.0 the system is Mott insulating. $2\Delta_o(p)$ relating to the induced superconducting condensation is represented by the vertical hatching, and maximizes close to $p = 1/6$ at around 40 meV in YBCO. For a representation of how $\mathcal{U}$ changes with **k** vector around the Fermi surface both as a function of p and of the system covalence see figure 4 in [17].

2. Understanding the Raman spectra of HTSC materials

Raman spectra provide a register both of electron–phonon scattering and of carrier–carrier electronic scattering. Phonon scattering has revealed some useful information and has provided a valuable complement to neutron scattering in assessing the unusual soft mode behaviour evident in the HTSC phenomenon. I do not wish to go back into this interesting and illuminating area, discussed at length in [15] in the light of the neutron results from Chung *et al* [30] and Pintschovius *et al* [31], but shall dwell here on the continuum electronic scattering below 800 cm^{-1} (100 meV). This too has been known from early times in the HTSC saga to be unusually structured [32, 33], showing characteristically varied behaviour for the B_{1g}, B_{2g} and A_g symmetry spectra. There arise interesting temperature and frequency variations and spectral scalings that make it evident the scattering processes which they record lie at the heart of the HTSC problem. The theory of electronic Raman spectroscopy is laid out in [2] and it suffices to appreciate now for the pseudo-tetragonal material that the B_{2g} (or XY) spectra will be most sensitive to inelastic scattering in the vicinity of the nodal direction in the HTSC cuprates, whilst the B_{1g} (or $X'Y'$) spectra emphasize inelastic scattering around the antinodal regions. Accordingly we expect from our earlier discussions that the latter spectra primarily will capture the formation and subsequent break up of local pairs, whilst the former will in the main monitor the pairing induced in the Fermi sea by the local pairs, i.e. they chiefly are going to yield information on $\mathcal{U}(p)$ and on $\Delta(p)$, respectively. Because the induced superconductivity bears closer numerical relation to T_c, it is the B_{2g} spectra that generally have become associated with superconductivity, leaving the B_{1g} spectra in a rather anomalous role. However, as we shall see, the B_{1g} spectra manifest all the desired characteristics to be associated with the local pairs and thus are intimately concerned with the sourcing of the global superconductivity.

Let us look at a list of attributes of the B_{1g} electronic Raman spectrum below 1000 cm^{-1} that are forthcoming from [32, 33] and the illuminating new release by Munnikes [34].

(i) There occurs a slowly saturating background continuum of scattering across this entire energy range that does not change greatly with T for $T > T_c$.

(ii) Below T_c appreciable spectral weight is lost from its low energy range below around 250 cm^{-1} (30 meV) to become, in optimally and moderately overdoped material, peaked up around 300–600 cm^{-1} (35–70 meV), details here being dependent upon doping and $T_c(p)$.

(iii) In underdoped material the above peak's *energy* does not fall away with reduction in p and $T_c(p)$, but goes on rising in value as p goes down.

(iv) The peak's *amplitude* (over and above the normal state scattering) rapidly fades away however into the underdoped region.

(v) In overdoped material, in contrast, the energy of the peak formed below T_c diminishes with increase in p value in a manner now roughly similar to $T_c(p)$ itself. Conversely, the *amplitude* of the peak scattering diverges as the peak *energy* recedes with $T_c(p)$ to zero around $p \sim 0.27$ [34].

(vi) The peak energy in overdoped material falls off in fact somewhat more rapidly than does $T_c(p)$, thereby destroying the scaling of $\hbar\Omega_{pk}$ to kT_c exhibited by optimally and slightly underdoped samples. (N.B. for the B_{2g} spectra there exists a complete scaling between $\hbar\Omega_{pk}$ and kT_c.)

(vii) Above T_c the background continuum spectral intensity, across all ω, fits to photon scattering from a *single-boson* entity [33]. This behaviour is to be contrasted with the two-boson variance in the two-magnon scattering in evidence at higher energies for strongly underdoped, insulating material.

(viii) Below T_c there is not sufficient low energy spectral weight change in these B_{1g} IR spectra to match a standard superconducting transition, it appearing as if a substantial number of quasiparticles remain ungapped [33].

Let us make now some further comments on the above same points.

(i) There is note no linear-in-ω intensity fall-off to low energies able to be attributed to anything other than the Bose factor; in particular there is no indication here of the Marginal Fermi Liquid behaviour that was evident in the A_{1g} and B_{2g} spectra.

(ii) The often rather analogous changes found in the B_{2g} spectra would uphold, nonetheless, some close tie-in of B_{1g} events to the superconductivity.

(iii) This rise in B_{1g} peak energy is precisely the form of change noted earlier for $\mathcal{U}(p)$ as the binding energy below E_F of the local pair state grows (see figure 1).

(iv) The peak amplitude fades away as the withdrawing negative-U state rapidly decouples from the free quasiparticles.

(v) Through the over doped system the value of $\mathcal{U}(p)$ diminishes until the negative-U state becomes unbound. By this level of doping ($p \approx 0.27$) screening has become very high, all pair lifetimes are now very short, and the photon scattering diverges in amplitude under pair dissolution.

(vi) The strong coupling physics, that at lower doping pushed both $\mathcal{U}(p)$ and $T_c(p)$ to high values, is replaced here by much weaker coupling behaviour, and the scaling ratio between kT_c and $\hbar\Omega_{pk}$ drops back towards a d-wave mean-field-like value for $\hbar\Omega_{pk}/kT_c$ of 4.3, rather than it being as in optimally and underdoped material up around 5.5–6 in the B_{2g} spectra, and even higher in B_{1g} (up to 9).

(vii) The assessed bosonic form to the thermal dependence of the scatterer responsible for the B_{1g} spectra is well matched by negative-U local pairs, in a way that the other 'localized entities' mooted find much more problematic.

(viii) As was indicated by the μSR work of Uemura *et al* [27], the cuprate superconducting condensation is not classical, it no longer simultaneously engaging all the carriers once below T_c. Moreover as the electronic specific heat work [28] makes apparent, transient local pairing persists to far above T_c; HTSC is not driven in the BCS fashion.

(ix) A further final point remains. Electronic events become impervious to standard temperatures at excitation energies beyond $\sim$800 cm^{-1} (or 100 meV). Above this energy there occurs merger of the 'normal' and superconducting state Raman spectra. This however does not mean that the local pairs vanish once $T > 300$ K: in all cases we are left with the abnormal structureless background scattering clearly extending through to remarkably high energies in excess of 1 eV. This scattering sources the Marginal Fermi Liquid behaviour, widely in evidence elsewhere in transport and ordinary IR optical spectroscopy.

What now of the B_{2g} and A_{1g} electronic Raman spectra? How do they fit in?

First let us turn to examine the A_{1g} spectra and what is revealed of the underlying physics disclosed in this polarization by addressing the second new Raman paper from Masui *et al* [35]. This work again concentrates upon optimally and overdoped material and deals with the system $(Y/Ca)Ba_2Cu_3O_{7-\delta}$. The usage here in Y-123 of such Ca substitution permits distinction to be made between those results which are a direct consequence of the hole doping content p and those that are to be attributed to the active participation of the structural chains in shaping the crucial behaviour in the planes. First point to note is that the A_{1g} peak energy and peak intensity, as for the B_{1g} spectra, strongly register a discontinuity at $p = 0.185$. Although referred to throughout [35] as occurring at $p = 0.19$, the data collection is sufficiently detailed to make identification here with $p = 0.185$ (for which I have my own reasons, laid out in [14, section 4.3]). The comparably sharp discontinuity witnessed at this same composition in the anisotropic resistive scattering work on $(La/Sr)_2CuO_4$ from [24] allows one to understand how the discontinuity, (first universally established at such p via electronic specific heat analysis [28], and there designated as 'pseudogap onset') is to be associated with the termination of full quasiparticle coherence. This coherence loss has been presented in [5d, 23] by the current author as being incurred under negative-U local pair creation and the ensuing quasiparticle scattering by those resonant pairs. Coherence is, in consequence, in jeopardy first within the antinodal regions, but steadily spreads towards the nodal regions as p is further reduced. The current Raman work actually indicates that in YBCO incoherence sets in slightly earlier perpendicular to the chains than occurs parallel to them, the result of inferior 3D coupling (see figure 4 in [35]). However by $p = 0.185$ the peak behaviours for both YY and XX polarizations have become identical, and the A_{1g} peak is there at its most pronounced. For higher p the A_{1g} and B_{1g} peaks had been indistinguishable, but now with $p = 0.185$ something of great import arises, as figure 2 (based upon figure 2 of [35] but augmented now by lines to guide the eye) will reveal. At this juncture the two peaks separate. The B_{1g} peak runs away up toward higher energies $\sim$70 meV, whilst the A_{1g} peak following a step increase in energy from 30 meV holds to a much lower trajectory that maximizes along with T_c at $p = 0.16$ at an energy of about 40 meV. If we are to associate the B_{1g} peak with individual local pairs and binding energy $\mathcal{U}(p)$, then we shall associate the A_{1g} peak with the superconducting

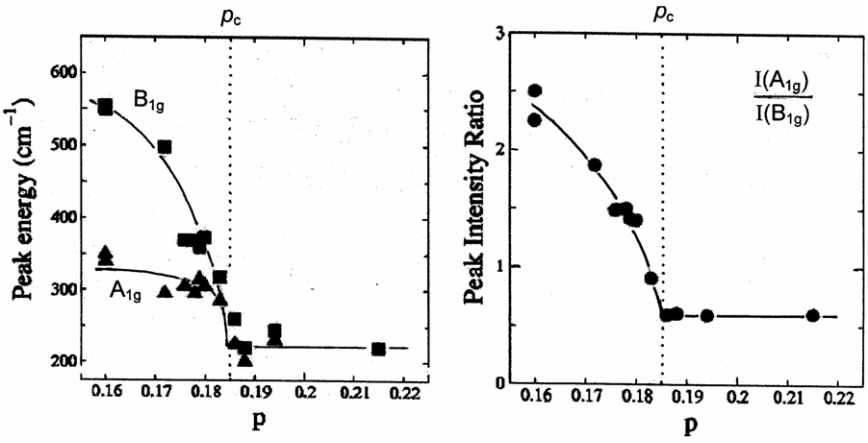

Figure 2. Development of figure 3 from [35] by Masui *et al*, indicating the evolution of the location of the low temperature peaks in the A_{1g} and B_{1g} electronic Raman spectra across a range of p values from optimally doped to quite highly overdoped samples of $(Y_{1-x}Ca_x)Ba_2Cu_3O_{7-\delta}$. The p values have here been generated using various combinations of x and δ, and the final behaviour shown to depend solely on p itself, not on x or δ individually. The A_{1g} and B_{1g} spectra come together above the critical value $p_c = 0.185$ (see [14, 23, 24] for significance of this doping level). Below p_c the B_{1g} spectra, which track the local pair binding energy, display a strong increase in Raman scattering peak excitation *energy* towards lower p, but it is the A_{1g} peak that grows there in relative *intensity*, as the electronic screening diminishes with increasing loss of quasiparticle coherence below p_c under the chronic e/b scattering. Note the high level of noise on the primary data of figure 2 in [35], and the fact that the phonon spectra have to be subtracted out, make precise identification of these electronic Raman peak energies difficult to specify to better than 40 cm^{-1} (or 5 meV).

condensate as engendered by the local pairs. The observed peak energy of 41 meV attained at optimal doping supports the earlier claim that the so-called neutron resonance peak, so prominent for p^{opt} at this energy, is to be associated with a spin-flip excitation within the condensate from the spin-singlet to the spin-triplet condition. Such a process effects the immediate dissociation of any local pair involved since the two parallel spins no longer can quantum mechanically be accommodated within the same locality [15, section 3]. Towards lower p and lower T_c the A_{1g} peak quite quickly fades away to become replaced as dominant feature by the B_{2g} peak. The latter tracks the residue of induced d-wave superconductive coupling, associated more and more with the nodal quasiparticles now, as interaction with the receding negative-U state diminishes.

The maximization of the A_{1g} peak intensity at $p = 0.185$, right where the superconductive energy is greatest, emphasizes the driving role of the local pairs in procuring HTSC behaviour. This sharp growth in amplitude of the A_{1g} peak (relative to the B_{1g} peak [35, figure 3(b)]) is a marker of the fact that the A_{1g} symmetry susceptibility is much the more subject to electronic screening [36]. This point was made early on by Cardona and co-workers [37] when, via fine tuning the A_{1g} *phonon* line across T_c by running through the full gamut of rare-earth substitutions, it was first possible to pinpoint the superconducting gap energy. The presently observed (much larger) step adjustment in the electronic Raman peak to higher *energy* as one transits through the coherence limit at $p = 0.185$ expresses once again the sensitivity of the A_{1g} symmetry signal to decrease in electronic screening. It is evident from figure 2 that if this step up in A_{1g} peak energy could be enhanced one might expect T_c(opt) to be enhanced. That is what in fact it would seem occurs as one manipulates the counter-ions involved in these systems: as for example in turning to the divalent Hg systems from the higher-valent and lone pair containing Tl-, Pb- and Bi-based systems. Similarly some substitution of oxygen by more ionic fluorine would look to be a move in the same direction as is borne out by the largest T_c reported to date coming from fluorine substituted Hg-1223 [38].

Finally a word about the B_{2g} spectra. These nodally active spectra do not change greatly in amplitude with doping and their behaviour throughout reflects immediate association with the superconducting condensate. Unlike with B_{1g}, there exists full and universal scaling between T_c-normalized spectra over all ω, $\hbar\Omega_{pk}/kT_c$ holding throughout to the strong coupling value of 5.5–6. Such a value is retained even as T_c falls with p to very low values. At *all* doping levels, as far as this mean-field, BCS-like, induced, more nodal component to the superconductivity is involved, HTSC stands the outcome of very strong and unusual coupling.

3. Understanding the infra-red optical spectra of HTSC systems

Study of the pair coupling in superconductors in traditional circumstances revolves around the function $\alpha^2F(\Omega)$, the electron–phonon spectral density function. In the present more complex case one can generalize this prescription to the form $I^2\chi(\Omega)$, relating to the 'active' bosonic spectral density, that may or may not involve retarded coupling. The interactions invoked do not directly manifest themselves in the optical (IR) spectra, but call for spectral inversion according to extended Drude, strong-coupling-type procedures. Strong characteristic features showing up in the real and imaginary parts of the optical conductivity are related to strong features in $I^2\chi(\Omega)$ that do not fall at quite the same energy.

The most advantageous mathematical fitting to extract the desired information from optical spectra is accomplished using the quantities the optical effective mass and the optical scattering rate. If one defines the optical self-energy $\Sigma^{\rm op}(T,\omega)$ relating to the optical conductivity via the equation

$$\sigma(T,\omega) = \frac{\omega_p}{4\pi}\frac{\mathrm{i}}{\omega - \Sigma^{\rm op}(T,\omega)},$$

then the real part of $\Sigma^{\rm op}(T,\omega)$ defines the relative optical effective mass $(m^{\rm op}/m^{\rm bare})$ via

$$\omega[(m^{\rm op}/m^{\rm bare}) - 1] = -2\Sigma_1^{\rm op}(T,\omega),$$

while the imaginary part of $\Sigma^{\rm op}(T,\omega)$ defines the optical scattering rate via

$$1/\tau^{\rm op}(T,\omega) = -2\Sigma_2^{\rm op}(T,\omega).$$

Note here the two-particle (e–h) optical scattering process will yield somewhat different information than does the single-particle scattering excitation experienced in photoemission.

Now what is the characteristic form taken by the HTSC IR spectra which for so long has perplexed researchers? The dominant feature characterizing both the real and imaginary parts of the experimental spectra is universally observed to sit at energies approaching *twice* that expected for $2\Delta_{\rm o}$ as elicited from other types of measurement. On the real side, the self-energy spectrum takes the form of a quite sharp peak, followed by a much broader, lower intensity hump. On the imaginary side, one finds a step edge, followed by steadily growing losses. While in both cases the broader aspects are retained to high temperature, the sharp features show up only below about $2T_{\rm c}$.

The new IR paper from [39] has reported such $E \perp c$ spectra from good quality, slightly underdoped Hg-1201 crystals ($T_{\rm c} = 91$ K), and they have followed through the necessary spectral inversion, employing a maximum entropy routine, to access the underlying initiating spectral function $I^2\chi(\Omega)$. While the experimental $m^{\rm op}(T,\omega)$ and $1/\tau^{\rm op}(T,\omega)$ plots display their characteristic changes up around 90 meV, it very tellingly emerges that the spectral coupling function responsible presents a very sharp peak back at 56 meV, this followed up by a weaker, much broader hump running out to high energy. This resonant feature in the coupling function at $\Omega_{\rm r} = 56$ meV still stands note considerably beyond the $2\Delta_{\rm o}$ superconducting gap energy of 45 meV appertaining to the slightly underdoped sample. One finds in addition that energy $\Omega_{\rm r}$ is effectively T-independent (see inset to figure 2 in [39]), while the appreciable thermal dependence of the resonance's amplitude and width proves quite un-phonon-like, the feature rapidly becoming less pronounced as T rises. All these observations support one, in light of what was developed in section 2, in making identification of the resonant feature in $I^2\chi(\Omega)$ with $\mathcal{U}(p)$, the negative-U state binding level.

Yang *et al* next provide the results of a comparable analysis for Hg-1223, employing earlier data, and reach appropriately scaled values of 130 K, 58 meV and 72 meV for $T_{\rm c}$, $\Delta_{\rm o}$ and $\Omega_{\rm r}$ respectively, the experimental spectral features in $1/\tau^{\rm op}$ and $m^{\rm op}$ now sitting for Hg-1223 up near 110 meV. Taking a whole range of approximately optimally doped materials these authors discover that $\Omega_{\rm r}/kT_{\rm c} \sim 6.3$—although the detailed values for $\Omega_{\rm r}(p)$ have to track $\mathcal{U}(p)$ if the above identification is correct. As is to be expected from section 2, the above quoted number of 6.3, given the (sub)optimal doping, is somewhat greater than the analogous ratio of 5.5 relating to the neutron spin resonance peak. The latter figure, recall, refers not to the binding energy of the local pairs *per se* but to the *overall* superconducting condensate (see figure 2).

The analysis of the electronic infra-red spectra has been advanced further in a very recent set of papers from van Heumen *et al* [40]. A direct attempt is made there to strip away all the more mundane thermal excitations for the bosons and fermions involved in the self-energy of the interaction process into a subsidiary multiplicative function so as to expose the fundamental frequency (and indeed ultimately temperature dependence) of the residual glue function. The latter now is labelled $\tilde{\Pi}(\omega,T)$ to express a more general regard for the actual interactions responsible for the witnessed self-energy changes. In particular, in regard to the resonance peak and the broader feature encountered beyond, an attempt is made to examine their individual characters. Are they both part of the pair-glueing operation, or does one in fact relate to pair forming and the other perhaps to pair breaking? It emerges that, while much of value can be recovered from the attempted customary strong coupling treatment of the results, there clearly is not full analogy here with what has been witnessed for phonon-mediated coupling, or indeed is anticipated for spin fluctuation coupling.

What is undertaken in the more exploratory of the three above papers [40c] is a comparison of the outcome of these new experiments with what could be expected if (i) marginal Fermi Liquid theory [3] were to prevail in the normal state, or (ii) the conditions implied by spin fluctuation theory held [41]. Neither of these in truth looks appropriate because of the rather structureless forms of $\tilde{\Pi}$ implicit, and it is only after an additional low energy Lorentzian rather artificially is introduced that any real matching can be achieved to experiment. A direct evaluation of the $\tilde{\Pi}$ glue function from experiment discloses, in contrast, quite distinct interactions proceeding in the far- and the mid-IR. By extracting the coupling constant λ from

$$\lambda = 2\int_0^{\omega c} \tilde{\Pi}(\omega)/\omega\,\mathrm{d}\omega,$$

it is possible to reach the following decomposition of $\lambda_{\rm total}$ for Hg-1201 at 295 K [40c]:

$$\lambda_{\rm total} = 1.85, \qquad \text{with } \lambda_{\rm FIR} = 0.7 \qquad \text{and} \qquad \lambda_{\rm MIR} = 1.2.$$

Note because of the narrowness of the FIR resonance feature that, as far as coupling goes, it stands as junior partner here. It exhibits considerable broadening, though, at lower temperatures towards lower energies, and it is this which largely is responsible for the significant temperature dependence of $\lambda_{\rm total}$. The latter mounts in $HgBa_2CuO_{4+\delta}$ from 1.85 at room temperature, to 2.0 at 200 K, to 2.3 by just above $T_{\rm c}$. Such values are very appreciably higher than the values for $\lambda \sim 0.3$–0.5 extracted from the nodal, low energy dispersion

kinks disclosed in ARPES work. Remember here however that optical spectroscopy is not k-sensitive and it automatically now will incorporate the antinodal response, wherein the current superconductive coupling activity is pre-eminent.

How then does one account for the above apparent dual aspect to the coupling function in the negative-U scenario? If the resonance feature bears the signature of those local pairs rendered external to the condensate, what is the 200–300 meV mid-IR feature all about? Clearly the latter lies way above the standard range of harmonic phonon energies, and, moreover, it exceeds what is relevant for magnetic coupling in the HTSC cuprates [42]. Pointedly it occurs precisely where the so-called 'waterfall' effect is found in ARPES work [43].

Let us reflect a little more closely upon the detailed nature of the local pairs in the present situation and upon how they are eliminated by optical excitation. The first stage is to unbind the negative-U pair relative to E_F; i.e. to supply the energy $\mathcal{U}(p)$ of the resonant feature. The second stage is to shake off the lattice energy change associated with the local structural relaxation incurred with double loading, i.e. when moving from $^{9}Cu_{III}^{1-}$ to $^{10}Cu_{III}^{2-}$. What this involved was the Jahn–Teller distorted, c-axis-elongated d^9 site in conversion to the spherical d^{10} closed shell condition. Additionally there occurred distension of the closed shell under the action of the (partially screened [4]) charge imbalance now between the local nuclear charge and the site's acquired electron complement. These effects bring substantial change to the lattice, long registered in measurements like EXAFS and PDF, or in isotopic T_c shifts, etc…. More recently we have had the very striking structural results from [44] and from Gedik *et al*—the latter being obtained using laser pump–probe crystallography [10, 12].

Now in the decomposition of the local pair we still have not finished because the pair yet has to be broken electronically; i.e. the correlation energy still has to be supplied to return the double-loading electron back into another coordination unit. In fact this is the major energy involved, and local pair disintegration stands accordingly not as a two-stage process but a three-stage process. It has been known for ten years or so that in all 1.5 eV per electron is demanded to see the pair revert back into two independent quasiparticles. Such information is forthcoming [11, 14] from two different sources (i) laser pump–probe optical spectroscopy [7–9], and (ii) thermomodulated, near-infra-red optical spectroscopy [13]. As was disclosed in the latter work by Little and co-workers, despite the $1/\omega$ factor much diminishing the contribution to λ issuing from such high energies, these near-IR excitations bring a further augmentation $\sim$0.35 to the λ values actually operative.

The question that raises itself now is how, in the presence of such large λ values, T_c can manage only to be as high as it is, rather than breaking through to the long sought target of 300 K. The answer has to lie in the fact that these systems are not homogeneous nor indeed fully coherent. Fermi Liquid theory no longer holds here, with basic scalings such as the Wiedemann–Franz law becoming non-classical as p progressively is reduced [45]. In particular, as regards the superconductivity, any direct application of the equations within the customary Eliashberg formalism must prove inadequate.

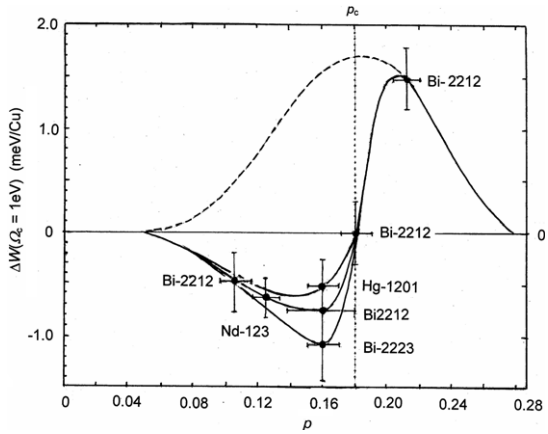

Figure 3. Amplification of figure 1 in [40c] from von Heumen *et al*, dealing with changes in spectral weight on cooling through T_c, as deduced from the low energy optical conductivity spectra for materials drawn from a variety of HTSC systems and distributed across a wide range of p value. As in figure 2, the critical p_c value of 0.18(5) manifests itself in striking fashion, being here where the low energy spectral weight change ΔW (cooling through T_c) very rapidly, if not discontinuously, changes sign. ΔW is here evaluated from the partial sum rule due to Ferrell, Glover and Tinkham connecting the amplitude of the superconducting condensate (at $\omega = 0$), the superfluid density ρ_s, to the integrated changes in $\sigma_1(\omega)$ across T_c $\rho_{s,r} = \int_{0+}^{\Omega} d\omega \{\sigma_{1,r}^{N}(\omega) - \sigma_{1,r}^{sc}(\omega)\}$. For classical superconductors the cut-off frequency Ω is typically only $\sim 5\Delta$, and in a one-band tight binding situation $\int \sigma_{1,r}(\omega)\, d\omega$ is proportional to the electronic kinetic energy decrease. By contrast in the present case a 1 eV cut-off has been imposed. Below p_c the data appear on separate traces dependent on whether for mono-layer, bi-layer or tri-layer material.

The optical work itself provides some indication of where this breakdown in standard strong coupling work is occurring and a glimpse too as to what may yet be done to elevate T_c further towards the great objective. By means of very careful FIR experimental and analytical investigation of the Drude limit, van der Marel and co-workers have demonstrated [46] that the spectral weight changes which arise in the cuprates across T_c are not in line with standard superconductive condensations. Normally on cooling below T_c not only does the potential energy fall (stabilize), but the quasiparticles also shed kinetic energy. However, by contrast, for the HTSC materials once below $p_c = 0.18$ they manifest what has been presented as an anomalous rise in K.E. when passing down through T_c, apparently this countering the fall in potential energy deriving from the superconductive condensation. Figure 3, based on figure 1 of [40c], sets out the extracted spectral weight change results for a whole range of HTSC systems and dopings. The envelopes have been sketched in here to draw out the systematics of what is being revealed. The upper envelope is a representation of what might be expected in a standard circumstance. The lower envelopes indicate that the sharp deviation from such behaviour clearly is centred upon $p = 0.185$. From the actual sign inversion witnessed here in ΔW and from the particular concentration involved, it would appear to the present author that interpretation of this development in terms of kinetic

energy change is not the correct avenue to follow. It becomes more appropriate to set the discussion in terms of loss of coherence within the 'normal' state, and of an ensuing loss of full-time participation of the full complement of electrons within the superconducting condensate. We have witnessed from the specific heat work [28] how the condensation energy tumbles below this p_c, how the superfluid density as revealed by the μSR work [27] fades away, and how the zero-frequency transport scattering is transformed there [24]. The deficit in kinetic energy registered below T_c must in part accordingly be due to the fact that it is not drawn from *all* the carriers in the customary way. Any worries about what high energy cut-off to employ in the spectral weight integral have on this count to stand without resolution. The unascertainable shortfall clearly is nonetheless in no way driver of or indeed marker for the superconductivity itself, since T_c shows no discontinuity at all at p_c. HTSC clearly thrives on action at the edge of incoherence, where metallic screening is weak and local pair formation and interaction are best advanced.

4. The illumination of events provided by $E \parallel c$ IR spectra

The above perception of the course of events is excellently endorsed in the very recent work from [47]. These researchers have chosen to concentrate on the c-axis polarized spectra, rather then on the much more metallic and less strongly structured basal-plane response recorded in the more usual $E \perp c$ polarization. To obtain accurate data off the vertical faces of the crystals is of course much more demanding than securing $E \perp c$ basal-plane spectra, but the $E \parallel c$ polarization proves particular sensitive to all c-axis coupling, and to coherence in general, whether for the normal or for the superconducting states. This high sensitivity may be tweaked further by the application of a magnetic field. Recognizing this, LaForge *et al* [47] have made a detailed spectral weight study for $YBa_2Cu_3O_y$ as a function of doping level, and contrasted the often quite slight but significant differences in spectral form coming when the reflectance experiments are carried out in magnetic fields of up to 8 T (whether with $H \parallel c$, as more normal, or $H \perp c$). That such changes and differences actually are registered under fields of this magnitude, far below H_{c2}, is marker of the fact that the primary deleterious effect of a magnetic field upon a superconductor is not as individual pair breaker, but as breaker of the phase coherence for the entire ensemble. The observation that the changes within the $H \parallel c$ and $H \perp c$ spectra may in places actually be rather large stresses the advantage of working in $E \parallel c$ polarization, for which all matters of coherence become ultra-sensitive when p is at and just below p_c.

Let us examine in some detail now what is being observed in these c-axis spectra. Firstly it should be recalled that due to the much-decreased metallicity in this direction the reflectance IR no longer is dominated by the Drude response and the phonons now stand out clearly. Below T_c, when the spectrum is strongly further modified by formation of the condensate, the general transfer of spectral weight to zero frequency uncovers the c-axis Josephson plasma resonance

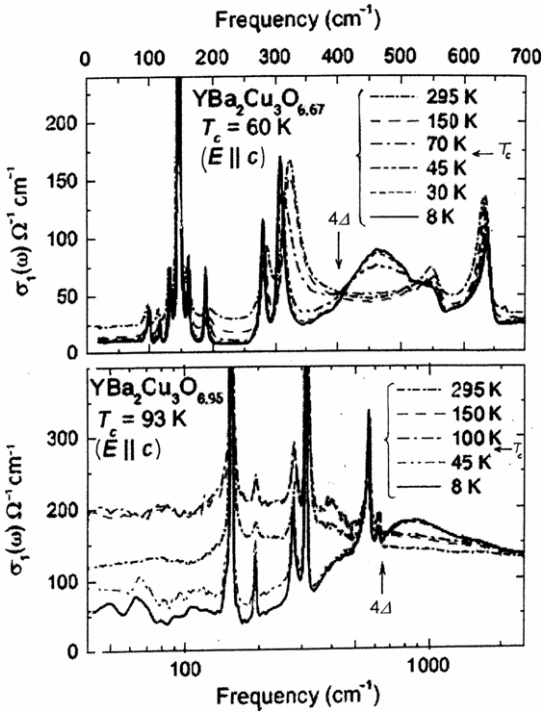

Figure 4. Real part of the optical conductivity for $YBCO_{6.67}$ and $YBCO_{6.95}$. Attention is drawn to the isosbestic intensity changes with temperature change across energies $4\Delta_o$. These points are marked by vertical arrows. Note the logarithmic frequency scale in the lower panel. Between 3Δ and 4Δ the intensity falls on cooling and is transferred up into the 4Δ–5Δ range. The figure is based on figure 5 of [47] and is for $H = 0$. (400 cm^{-1} $\equiv$ 50 meV.)

excitation for the condensate, as well as further collective excitations in the far-IR. From the frequency of the resonance, strongly in evidence in reflection, it is possible to obtain a direct measure of ρ_s itself for the sample via application of the equation $\omega_{JPR} = \sqrt{(\rho_s/\varepsilon_{\infty c})}$. ρ_s is derivable too from $\omega\sigma_2(\omega)$, and is naturally identical in both polarizations. The Josephson resonance occurs in the optimally doped sample at 250 cm^{-1} (31 meV) and at 60 cm^{-1} (7.5 meV) for their $y = 6.67$ sample. After conversion of $R(\omega)$ to $\sigma(\omega)$ by Kramers–Kronig methods it immediately becomes evident that the loss of spectral weight below T_c stretches not to 2Δ but through to 4Δ. This signals that the excitation edge is to be associated here not with pair breaking and the liberation of two unpaired carriers to E_F, but with the raising of a bound pair as a unit within the condensate into the upper Bogoliubov hole band, an excitation of 4Δ per pair. Above this energy a very interesting hump is registered. Below $T \approx T_c$, whether resulting from field or temperature change, there is evident in the spectra a clear isosbestic point at energy 4Δ (see figure 4) with a transfer of spectral weight from the region between 3Δ and 4Δ *up* into the range between 4Δ and 5Δ. In $YBCO_{6.67}$ the isosbestic 4Δ point sits at 50 meV (400 cm^{-1}) while in $YBCO_{6.95}$ it sits up at 80 meV (640 cm^{-1}). The hump developing between 4Δ and 5Δ has the appearance of a pseudo-phonon and clearly is related to the B_{1g} feature in the Raman spectra at this energy (figure 2), ascribed there to local pairs, these now excited free of the influence of the condensate to somewhat above E_F. In the optimally doped sample the spectral region indeed shifts

down to somewhat lower energy and also becomes suitably lowered in intensity (see [47], figures 5, 6 and 8).

Let us now look at some of the changes specifically wrought in these spectra by application of the magnetic fields. In underdoped material there is in evidence a marked shortfall, as noted above, between ρ_s as it directly is measured and the integrated spectral weight in $\sigma_1(\omega)$ as generated here by imposing integration cut-offs $\Omega_c \leqslant 10\Delta$ ($\sim$150 meV or 1200 cm^{-1}). Even for the relatively small fields used, $\rho_s(H)$ is universally observed to fall away very appreciably with $|H|$, in a manner akin to thermal excitation. There is, though, pointed distinction here compared with what is evaluated for $\Delta W(\Omega_c, H)$. ΔW under $H \parallel c$ moves to meet ρ_s quite quickly, but with $H \perp c$ it progressively decreases retaining its separation from ρ_s. This signals that high energy contribution to the spectral weight is not so damaged under the latter field orientation, for which the flux vortices do not lead to superconducting phase disorder between layers. These high energy contributions to both ΔW and ρ_s prove widely forthcoming to energies much greater than the upper 10Δ cut-off imposed. Locally around the isosbestic point, $H \perp c$ has a more marked effect upon spectral weight changes than does $H \parallel c$ ([47] figure 9). This implies that here there arises more than just loss of phase coherence: there occurs definite extensive transfer of optical spectral weight back out to higher energy. $H \perp c$ likewise produces a more striking effect upon the Josephson plasma resonance feature than does $H \parallel c$; the latter simply depresses ρ_s and ω_{JPR} somewhat, but $H \perp c$ institutes additional new resonances.

The observation that the primary effect of a magnetic field on superconductivity is to break phase coherence rather than actually to break pairs explains directly why all the above effects witnessed in these remarkably small fields are found to cease near T_c. Above T_c one still has the local pairs but these lack phase coherence. The fact that this general pattern is altered somewhat for the changes near the isosbestic point marks that those changes are intimately connected with the excitation itself, the local pairs being in course of transfer out of the body of the coherent condensate. The $E \parallel c$ experiments have accordingly yielded invaluable information about the nature and sustenance of the global condensate.

5. Conclusions

Very recent Raman and optical data dealing with optimal and somewhat hole-rich samples for a variety of HTSC systems have been examined closely from the negative-U, boson–fermion crossover point of view. These results all find ready accommodation within that framework; notably the contrasting development of A_{1g}, B_{1g} and B_{2g} polarized electronic Raman spectra with p and T, and the isosbestic nature of the thermal modification to the infra-red optical conductivity occurring about energy 4Δ. Both the Raman and IR spectra bear clear imprint of the changes due to quasiparticle incoherence setting in at $p = 0.185$, and precipitating marked changes in electrical transport behaviour, presently a renewed centre of interest. The origin of the incoherence has been presented as resulting from e-on-e to b resonant charged boson production and the ensuing e-on-b scattering, the latter becoming dominant as the sustained boson population maximizes. The maximum pair condensation energy occurs precisely as quasiparticle incoherence under this carrier scattering is encountered at $p = 0.185$. Metallic screening is then at a minimum, thereby permitting the establishment of the highest net pair population of local (negative-U) and induced carrier pairings. Magnetic field effects upon the level of superconductive coherency obtaining prove highly illuminating.

References

[1] Timusk T and Statt B 1999 *Rep. Prog. Phys.* **62** 61
[2] Devereux T P F and Hackl R 2007 *Rev. Mod. Phys.* **79** 175
[3] Varma C M 1989 *Int. J. Mod. Phys.* B **3** 2083
[4] Raebiger H, Lany S and Zunger A 2008 *Nature* **453** 763 (Note 'cation' charge integrations here confined to a 1.3 Å radius)
[5a] Wilson J A 1988 *J. Phys. C: Solid State Phys.* **21** 2067–102
[5b] Wilson J A 1989 *Int. J. Mod. Phys.* B **3** 691–710
[5c] Wilson J A 1994 *Physica* C **233** 332
[5d] Wilson J A and Zahrir A 1997 *Rep. Prog. Phys.* **60** 941–1024
[6] Wilson J A 2000 *J. Phys.: Condens. Matter* **12** R517–47
[7] Stevens C J, Smith D, Chen C, Ryan J F, Pobodnik B, Mihailovic D, Wagner G A and Evetts J E 1997 *Phys. Rev. Lett.* **78** 2212
[8] Demsar J, Hudej R, Karpinski J, Kabanov V V and Mihailovic D 2001 *Phys. Rev.* B **63** 054519
[9] Li E, Li J J, Sharma R P, Ogale S B, Cao W L, Zhao Y G, Lee C H and Venkatesan T 2002 *Phys. Rev.* B **65** 184519
[10] Gedik N, Yang D S, Logvenov G, Bozovic I and Zewail A H 2007 *Science* **316** 425
[11] Wilson J A 2000 *J. Phys.: Condens. Matter* **12** 303
[12] Wilson J A 2007 *J. Phys.: Condens. Matter* **19** 466210
[13] Little W A and Holcomb M J 2000 *J. Supercond.* **13** 695
[14] Wilson J A 2001 *J. Phys.: Condens. Matter* **12** R945–77
[15] Wilson J A 2004 *Phil. Mag.* **84** 2183
[16] Wilson J A 2007 *J. Phys.: Condens. Matter* **19** 106224
[17] Wilson J A 2008 *J. Phys.: Condens. Matter* **20** 385210
Wilson J A 2009 arXiv:0903.3549
[18] McElroy K, Lee J, Slezak J A, Lee D-H, Eisaki H, Uchida S and Davis J C 2005 *Science* **309** 1048
Alldredge J W *et al* 2008 *Nat. Phys.* **4** 319
[19] Hanaguri T, Kohsaka Y, Davis J C, Lupien C, Yamada I, Azuma M, Takano M, Ohishi K, Ono M and Takagi H 2007 *Nat. Phys.* **3** 865
Kohsaka Y *et al* 2008 *Nature* **454** 1072
[20] Hanaguri T, Kohsaka Y, Ono M, Maltseva M, Coleman P, Yamada I, Azuma M, Takano M, Ohishi K and Takagi H 2009 *Science* **323** 923
[21] Wilson J A 1997 *J. Phys.: Condens. Matter* **9** 6061
[22] Wilson J A 1972 *Adv. Phys.* **21** 143
[23] Wilson J A 2009 *J. Phys.: Condens. Matter* **21** 245702
[24] Cooper R A *et al* 2009 *Science* **323** 603
[25] Analytis J G, Abdel-Jawad M, Balicas L, French M M J and Hussey N E 2007 *Phys. Rev.* B **76** 104523
French M M J, Analytis J G, Carrington A, Balicas L and Hussey N E 2009 *New J. Phys.* **11** 055057
[26] Vignolle B, Carrington A, Cooper R A, French M M J, Mackenzie A P, Jadet C, Vignolles D, Proust C and Hussey N E 2008 *Nature* **455** 952
[27] Uemura Y J 2000 *Int. J. Mod. Phys.* B **14** 3703
[28] Loram J W, Luo J, Cooper J R, Liang W Y and Tallon J L 2001 *J. Phys. Chem. Solids* **62** 59
[29] Wilson J A 2008 *J. Phys.: Condens. Matter* **20** 015205
Chien C-C, He Y, Chen Q and Levin K 2009 *Phys. Rev.* B **79** 214527

[30] Chung J-H *et al* 2003 *Phys. Rev.* B **67** 014517
[31] Pintschovius L, Reznik D, Reichardt W, Endoh Y, Hiraka H, Tranquada J M, Uchiyama H, Masui T and Tajima J 2004 *Phys. Rev.* B **69** 214506
[32] Reznik D, Cooper S L, Klein M V, Lee W C, Ginsberg D M, Maksimov A A, Puchkov A V, Tartakovskii I I and Cheong S-W 1993 *Phys. Rev.* B **48** 7624
[33] Puchkov A V, Timusk T, Karlow M A, Cooper S L, Han P D and Payne D A 1996 *Phys. Rev.* B **54** 6686
[34] Munnikes N *et al* 2009 arXiv:0901.3448
[35] Masui T, Hiramachi T, Nagasao K and Tajima S 2009 arXiv:0901.0620
[36] Wenger F and Käll M 1997 *Phys. Rev.* B **55** 97
Cardona M 1999 *Physica* C **317/318** 30–54
[37] Friedl B, Thomsen C and Cardona M 1993 *Phys. Rev. Lett.* **65** 915
[38] Monteverde M, Núñez-Regueiro M, Acha C, Lokshin K A, Pavlov D A, Putilin S N and Antipov E V 2004 *Physica* C **408–410** 23
[39] Yang J, Hwang J, Schachinger E, Carbotte J P, Lobo R P S M, Colson D, Forget A and Timusk T 2009 *Phys. Rev. Lett.* **102** 027003
[40a] van Heumen E, Muhlethaler E, Kuzmenko A B, Eisaki H, Meevasana W, Greven M and van der Marel D 2009 *Phys. Rev.* **79** 184512
[40b] van Heumen E, Meevasana W, Kuzmenko A B, Eisaki H and van der Marel D 2009 *New J. Phys.* **11** 055067
[40c] van Heumen E, Kuzmenko A B and van der Marel D 2009 arXiv:0904.2502
[41] Barzykin V and Pines D 2009 *Adv. Phys.* **58** 1–65
[42] Hayden S M, Mook H A, Dai P, Perring T G and Dogan F 2004 *Nature* **429** 531
Woo H, Dai P, Hayden S M, Mook H A, Dahm T, Scalapino D J, Perring T G and Dogan F 2006 *Nat. Phys.* **2** 600
Vignolle B, Hayden S M, McMorrow D F, Rønnow H M, Lake B, Frost C D and Perring T G 2007 *Nat. Phys.* **3** 163
Lipscombe O J, Vignolle B, Perring T G, Frost C D and Hayden S M 2008 *Phys. Rev. Lett.* **102** 167002
Hinkov V, Bourges P, Pailhés S, Sidis Y, Ivanov A, Frost C D, Perring T G, Lin C T, Chen D P and Keimer B 2007 *Nat. Phys.* **3** 780
[43] Chang J *et al* 2007 *Phys. Rev.* B **78** 205103
[44] Röhler J 2004 *J. Supercond.* **17** 159
[45] Proust C, Behnia K, Bel R, Maude D and Vedeneev S I 2005 *Phys. Rev.* B **72** 214511
[46] van Heumen E *et al* 2007 *Phys. Rev.* B **75** 054522
[47] LaForge A D, Padilla W J, Burch K S, Li Z Q, Schafgans A A, Segawa K, Ando Y and Basov D N 2009 *Phys. Rev.* B **79** 104516